AGU PUBLICATIONS

JGR

Journal of Geophysical Research: Earth Surface

RESEARCH ARTICLE
10.1002/2013JF003009

Key Points:
- Glaciers in the Southern Alps are sensitive to precipitation distribution
- The New Zealand Last Glacial Maximum was 8.25°C to 5.5°C cooler than present
- Glacier models should estimate an envelope of paleoclimate variability

Correspondence to:
A. V. Rowan,
annr@bgs.ac.uk

Citation:
Rowan, A. V., S. H. Brocklehurst, D. M. Schultz, M. A. Plummer, L. S. Anderson, and N. F. Glasser (2014), Late Quaternary glacier sensitivity to temperature and precipitation distribution in the Southern Alps of New Zealand, *J. Geophys. Res. Earth Surf.*, *119*, 1064–1081, doi:10.1002/2013JF003009.

Received 10 OCT 2013
Accepted 7 APR 2014
Accepted article online 11 APR 2014
Published online 9 MAY 2014

Late Quaternary glacier sensitivity to temperature and precipitation distribution in the Southern Alps of New Zealand

Ann V. Rowan[1,2], Simon H. Brocklehurst[3], David M. Schultz[3], Mitchell A. Plummer[4], Leif S. Anderson[5], and Neil F. Glasser[1]

[1]Centre for Glaciology, Department of Geography and Earth Sciences, Aberystwyth University, Aberystwyth, UK, [2]Now at British Geological Survey, Environmental Science Centre, Nottingham, UK, [3]School of Earth, Atmospheric and Environmental Sciences, University of Manchester, Manchester, UK, [4]Idaho National Laboratory, Idaho Falls, Idaho, USA, [5]Institute of Arctic and Alpine Research, and Department of Geological Sciences, University of Colorado Boulder, Boulder, Colorado, USA

Abstract Glaciers respond to climate variations and leave geomorphic evidence that represents an important terrestrial paleoclimate record. However, the accuracy of paleoclimate reconstructions from glacial geology is limited by the challenge of representing mountain meteorology in numerical models. Precipitation is usually treated in a simple manner and yet represents difficult-to-characterize variables such as amount, distribution, and phase. Furthermore, precipitation distributions during a glacial probably differed from present-day interglacial patterns. We applied two models to investigate glacier sensitivity to temperature and precipitation in the eastern Southern Alps of New Zealand. A 2-D model was used to quantify variations in the length of the reconstructed glaciers resulting from plausible precipitation distributions compared to variations in length resulting from change in mean annual air temperature and precipitation amount. A 1-D model was used to quantify variations in length resulting from interannual climate variability. Assuming that present-day interglacial values represent precipitation distributions during the last glacial, a range of plausible present-day precipitation distributions resulted in uncertainty in the Last Glacial Maximum length of the Pukaki Glacier of 17.1 km (24%) and the Rakaia Glacier of 9.3 km (25%), corresponding to a 0.5°C difference in temperature. Smaller changes in glacier length resulted from a 50% decrease in precipitation amount from present-day values (−14% and −18%) and from a 50% increase in precipitation amount (5% and 9%). Our results demonstrate that precipitation distribution can produce considerable variation in simulated glacier extents and that reconstructions of paleoglaciers should include this uncertainty.

1. Introduction

Glacial geology is an important terrestrial record of past climate change [e.g., *Kaplan et al.*, 2010; *Putnam et al.*, 2010]. Paleoclimate conditions can be inferred from this record using equilibrium line altitude (ELA) reconstructions based on mapping of paleoglacier shape [e.g., *Porter*, 1975] or using ice flow models that determine glacier volume [e.g., *Anderson and Mackintosh*, 2006; *Doughty et al.*, 2013; *Kaplan et al.*, 2013]. While both methods have advantages and disadvantages, the accuracy of the inferred paleoclimate is limited by the challenge of representing mountain meteorology in glacier models. Describing the spatial and seasonal variations of an essentially unchanging climate and the temporal changes in climatic conditions that are likely to affect the glacier balance also presents potential difficulties to model applications. Near-surface air temperature and precipitation rates are typically assumed to have a linear relationship with altitude, but the interaction of air masses with high topography modifies the distribution of precipitation. Reconstructions of glaciers located in the temperate, westerly dominated midlatitudes—for example, the Patagonian Andes [*Glasser et al.*, 2005; *Kaplan et al.*, 2008] and the Southern Alps of New Zealand [*Anderson and Mackintosh*, 2006; *Rother and Shulmeister*, 2006; *Golledge et al.*, 2012; *Rowan et al.*, 2013]—reveal compelling evidence for glacier sensitivity to both temperature and precipitation distribution.

The interaction between rugged, evolving topography and variable air circulation patterns is complex, and the distribution of precipitation in mountainous regions is often difficult to predict. Precipitation peaks do not correlate with the highest topography [*Henderson and Thompson*, 1999; *Schultz et al.*, 2002; *Steenburgh*, 2003; *Roe*, 2005; *Anders et al.*, 2006], and observations are scarce, as high-elevation rain gauges are frequently lacking, and these data typically only represent short time spans [*Groisman and Legates*, 1994]. Moreover,

precipitation amount, spatial distribution, temporal distribution, and phase will vary with climate change, so present-day precipitation data may not represent conditions during a glacial. As a result, the representation of precipitation in glacier models may be unsatisfactory and could result in unaccounted-for uncertainties in paleoclimate reconstructions [*Rother and Shulmeister*, 2006]. Seasonality in lapse rate [*Doughty et al*., 2013], air temperature, and precipitation amount [*Golledge et al*., 2010] may also modify mass balance. Many glacier modeling studies use summer-winter climatologies that do not consider the detail of these seasonal variations in meteorological variables. Furthermore, many glacier-modeling studies assume that glaciers were in equilibrium with the long-term mean values of temperature and precipitation amount. However, because glaciers also respond to interannual climate variations (climate noise), this assumption is likely to be invalid [*Anderson et al*., 2014].

The purpose of this paper is to quantify variations in the extents of reconstructed glaciers resulting from a realistic range of precipitation distributions for the Southern Alps of New Zealand. We apply two glacier models to the eastern Southern Alps to demonstrate the need for more realistic representations of orographic patterns of rain and snowfall. We consider whether these glacier reconstructions are precise indicators of past climate change, or if a more realistic approach is to quantify glacier sensitivities to climate and use these to infer an envelope of likely paleoclimate change—an approach previously used by *Anderson and Mackintosh* [2006] and *Golledge et al*. [2012] for temperature and precipitation amount. Our paper builds on these previous studies to quantify uncertainties in simulated glacier extents due to precipitation distribution, precipitation phase, interannual climate variability, and seasonality.

1.1. The Southern Alps

The Southern Alps of New Zealand (Figure 1) are an excellent location to explore the climate sensitivity of glaciers [*Oerlemans*, 1997; *Anderson and Mackintosh*, 2006; *Anderson et al*., 2010; *Putnam et al*., 2010; *Doughty et al*., 2013]. This 400 km long, ~120 km wide, northeast-southwest trending mountain range has summit elevations exceeding 3000 m [*Tippett and Kamp*, 1995; *Willett*, 1999]. The axial trend of the range is perpendicular to the prevailing westerly winds, resulting in a steep west-east precipitation gradient. The central Southern Alps experience extremely high precipitation of up to 14 m per year on the western (upwind) side of the range, which decreases rapidly to the east [*Henderson and Thompson*, 1999; *Wratt et al*., 2000]. The trend in ELA is strongly influenced by this precipitation gradient [*Chinn*, 1995], suggesting that orographic precipitation exerts a primary control on glaciation [*Porter*, 1975].

New Zealand is one of few landmasses in the southern midlatitudes, and paleoclimate reconstructions from New Zealand are important for comparison with global records [e.g., *Kaplan et al*., 2010; *Putnam et al*., 2012]. The Last Glacial Maximum (LGM) occurred in New Zealand between 24 and 18 ka [*Putnam et al*., 2013b]. The late Quaternary geology is well preserved and records frequent and rapid climate change [*Alloway et al*., 2007; *Barrell et al*., 2011]. There is little regional variation in bedrock lithology [*Cox and Barrell*, 2007], so glaciers are unlikely to be modified by their geological setting. Numerical simulations of the Southern Alps icefield [*Golledge et al*., 2012], the Ohau [*Putnam et al*., 2013b], the Pukaki [*McKinnon et al*., 2012], and the Rakaia [*Rowan et al*., 2013] Glaciers (Figure 1) demonstrated that LGM mean annual air temperature was between 6°C and 8°C cooler than present-day values and may have been accompanied by a reduction of up to 25% in precipitation.

1.2. Applications of Glacier Models in the Southern Alps

Previous glacier modeling studies in the Southern Alps have focused on the Franz Josef Glacier (Figure 1) to examine the climate sensitivity of this glacier [*Oerlemans*, 1997] and the drivers of the advance to the well-preserved Waiho Loop moraine [*Anderson and Mackintosh*, 2006; *Anderson et al*., 2008; *Alexander et al*., 2011]. *Oerlemans* [1997] and *Anderson and Mackintosh* [2006] demonstrated that differences in temperature rather than precipitation amount were the major control on the length of this glacier, but that high precipitation values enhanced temperature sensitivity; *Oerlemans* [1997] showed that the Franz Josef Glacier receded 1.5 km per °C of warming, whereas *Anderson and Mackintosh* [2006] showed that the glacier advanced at a rate of 3.3 km per °C of cooling. This difference was attributed to Oerlemans' unrealistically low precipitation values [*Tovar et al*., 2008; *Shulmeister et al*., 2009; *Alexander et al*., 2011]. Energy-balance calculations for the Brewster Glacier indicated high temperature sensitivity; a 50% change in precipitation amount was required to offset a temperature difference of 1°C [*Anderson et al*., 2010].

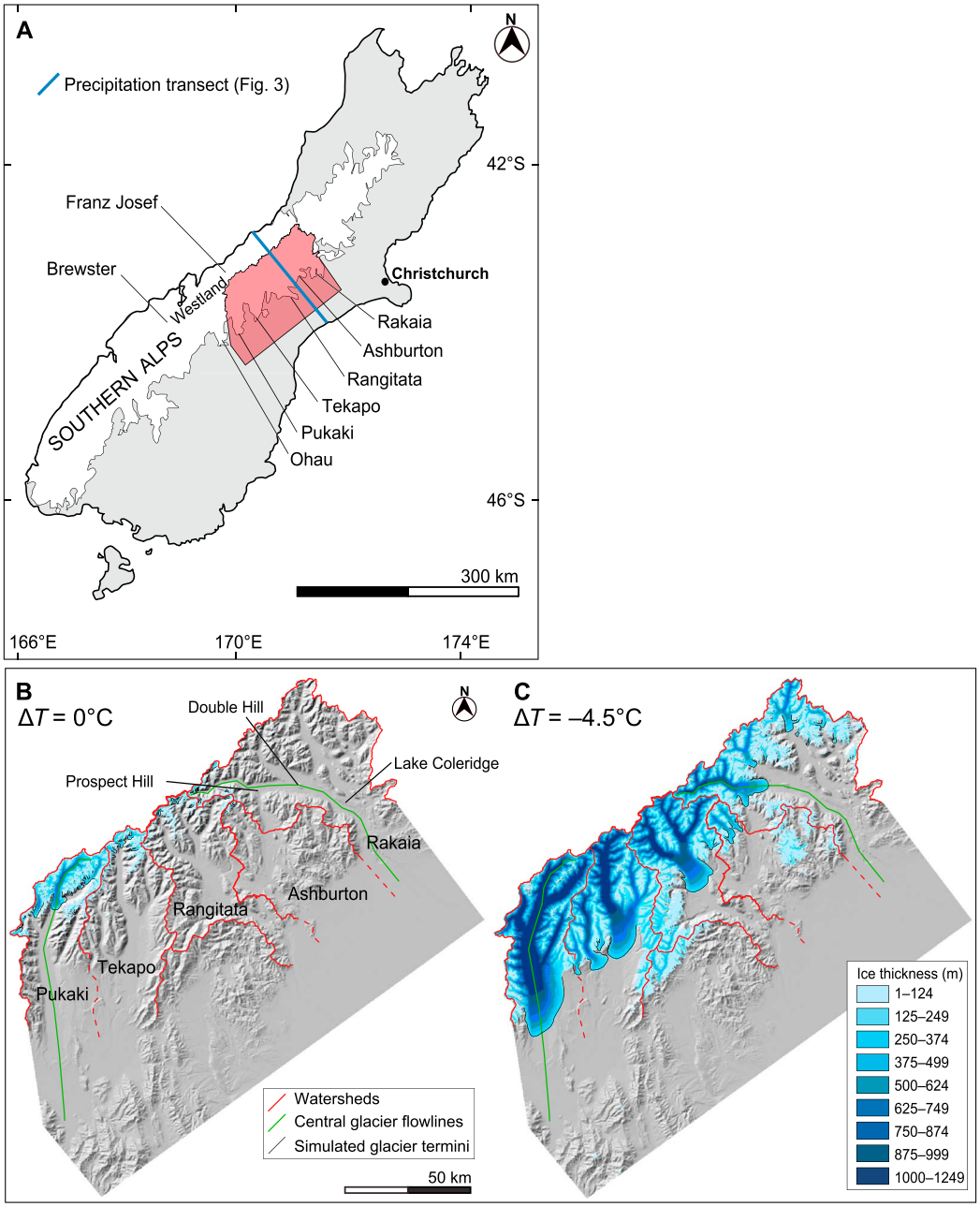

Figure 1. (a) Location of the study area in the Southern Alps of New Zealand, showing the model domain used in the 2-D experiments (red-shaded area), the maximum glaciated extent during the LGM (white shading), and location of the precipitation transect shown in Figure 3 (blue line). Glacier volumes simulated under (b) the present-day ($\Delta T = 0$°C) scenario (the baseline model), and (c) the Double Hill scenario ($\Delta T = -4.5$°C), overlain on a shaded relief map of the model domain. Catchment boundaries (solid red lines; dashed sections indicate interpretation over areas of low relief) and the flowlines used to measure length of the Pukaki and Rakaia Glaciers (solid green lines) are shown.

The Pukaki Glacier has a greater temperature sensitivity than the Brewster Glacier; an 82% increase in precipitation amount is required to offset a temperature difference of −1°C [*Anderson and Mackintosh*, 2012], probably due to the difference in the hypsometry of these glaciers. There may be uncertainty in simulated glacier extents due to bed geometry and subglacial erosion independent of climate change. A flowline model of the Pukaki Glacier indicated that variations in the bed topography could have forced kilometer-scale variation in glacier length to form the two distinct LGM moraine sequences in this valley [*McKinnon et al.*, 2012].

Table 1. Two-Dimensional Glacier Model Parameter Values Used in the Simulations Described in This Paper

	Values
Model Domain Description	
Native horizontal grid spacing of LINZ DEM (m)	50
Vertical precision of LINZ DEM (m)	1
Cell size of model domain (m)	200
Model domain grid (number of cells)	571 × 528
Glaciological parameters	
High albedo	0.74
Low albedo	0.21
Maximum slope that can hold snow (degrees)	30
Slope increment for avalanching routine (degrees)	12
Minimum new snow for avalanching to occur (m SWE)	0.1
Deformation constant (yr^{-1} kPa^{-3})	2.10×10^{-7}

The poor fit of some simulated glaciers to mapped moraines, particularly when the model features more than one glacier, indicates the need to quantify the uncertainties associated with the application of glacier models to avoid misleadingly precise paleoclimate estimates. In a model reconstruction of glaciers in the eastern Southern Alps, the Rakaia Glacier was underrepresented by the LGM simulation that provided the best fit to the geological data compared to the neighboring Rangitata and Ashburton Glaciers [*Rowan et al*., 2013]. A model reconstruction of the Southern Alps LGM icefield generally provided a good fit to the glacial geology, although for some glaciers including the Rakaia, this simulation underestimated the LGM terminus positions [*Golledge et al*., 2012]. Increasing the simulated length of the Rakaia Glacier to reach the LGM extents required either further cooling of −0.25°C from an LGM simulation with a temperature difference of −6.5°C and no change in precipitation amount from present-day values [*Rowan et al*., 2013], or further cooling of −1.75°C from an LGM simulation with a temperature difference of −6.25°C and a 25% reduction in precipitation amount from present-day values [*Golledge et al*., 2012].

2. Methods

2.1. The 2-D and 1-D Glacier Models

We applied a 2-D energy-mass balance and ice flow model implementing the shallow-ice approximation [*Plummer and Phillips*, 2003] and a 1-D shallow-ice approximation flowline model [*Roe and O'Neal*, 2009] to catchments in the eastern Southern Alps (Figure 1). We used the 2-D model to investigate how temperature and precipitation modify the energy balance and extents of these glaciers, while the 1-D model was used for experiments investigating fluctuations in glacier length forced by interannual climate variability [cf. *Anderson et al*., 2014]. The 2-D glacier model has previously been applied to glaciers in the USA [*Plummer and Phillips*, 2003; *Laabs et al*., 2006; *Refsnider et al*., 2008] and New Zealand [*Rowan et al*., 2013; *Putnam et al*., 2013a]. These glacier models are based on the shallow-ice approximation developed for large ice sheets with shallow bed topography [*Hutter*, 1983], which is unsuitable for glaciers with dominantly steep bed topography [*Le Meur et al*., 2004]. Previous studies have successfully applied the shallow-ice approximation to glaciers in New Zealand [*Anderson and Mackintosh*, 2006; *Rowan et al*., 2013] and elsewhere [*Oerlemans et al*., 1998; *Kessler and Anderson*, 2006; *Refsnider et al*., 2008], and we consider this approximation valid for the large, low-angle valley glaciers that occupied the eastern Southern Alps.

The model domain includes the Rakaia to the Pukaki valleys (Figure 1). The Land Information New Zealand (LINZ) 50 m digital elevation model (DEM) was resampled to a 200 m grid spacing to describe topography (Table 1). Present-day ice volumes were removed from the DEM before applying the glacier models following the method of *Golledge et al*. [2012] using glacier outlines defined by LINZ and assuming a uniform basal shear stress (τ_b) of 150 kPa

$$H = \tau_b / (\rho^* g^* \sin \alpha), \quad (1)$$

where H is ice thickness, ρ is the density of pure glacier ice (917 kg m^{-3}) [*Cuffey and Paterson*, 2010], g is acceleration due to gravity (9.81 m s^{-1}), and α is the glacier surface slope taken from the resampled DEM. Model parameter values followed *Rowan et al*. [2013] for the Rakaia-Rangitata Glaciers (Tables 1 and 2). After an initial simulation for a particular temperature difference, the simulated glaciers were added to the DEM to iteratively recalculate mass balance across the glacier allowing for the increase in surface elevation with greater ice volume. Calculated mass balance and DEM topography were used as inputs to the ice flow model to calculate ice thickness. Results from the ice flow model were considered acceptable when the integrated mass balance (the difference between accumulation and ablation across the entire glacier) was within 5% of steady state.

Table 2. Variables Used in the Simulations Described in This Paper Following *Rowan et al.* [2013]

Climatological Variables	Annual	Summer	Winter
Monthly sea level temperature range (°C)	5.6–15.8	10.7–15.8	5.6–11.2
Standard deviation of daily temperature (°C)	2.9	3.1	2.7
Lapse rate (°C km^{-1})	−6		
Critical temperature for snowfall (°C)	2		
NIWA annual rainfall maximum (mm)	8450		
NIWA annual rainfall minimum (mm)	645		
NIWA annual rainfall mean (mm)	1602		
Wind speed ($m\,s^{-1}$)	3.2	3.6	2.8
Base wind speed elevation (m)	457		
Multiplier for wind speed increase with elevation	0.0008		
Cloudiness (fraction of sky obscured)	0.7		
Relative humidity (%)	77	75	79
Turbulent heat transfer coefficient (−)	0.0015		
Ground heat flux ($W\,m^{-2}$)	0.1		

We tested the variability in glacier volume from a baseline model of the present-day climate resulting from; uniform differences in mean annual air temperature (hereafter referred to as temperature), for example, present-day mean annual air temperature minus 1°C (hereafter ΔT); and multiplicative differences in precipitation amount, for example, 75% of present-day precipitation amount (hereafter P). Temperature difference is defined here as an increase or decrease in temperature calculated as 30 year means from daily measurements. Elsewhere in the glaciological literature, temperature difference may be referred to as "temperature change," implying variation in temperature throughout each simulation.

2.2. Climatological Data

The climate inputs to our baseline model (Tables 1 and 2) were based on 123 automatic weather stations (AWS) in the national climate database CliFlo (http://cliflo.niwa.co.nz/). We used 30 year (1971–2000) monthly mean and daily standard deviation values for temperature, monthly means for relative humidity and wind speed, and 30 year mean annual values for cloudiness. Although interannual variability was observed in the meteorological data, we used 30 year mean values as input to the 2-D model, as variations in climate with a shorter period than the glacier's response time are unlikely to produce the magnitude of length fluctuations we are examining (10–80 km length fluctuations).

In the baseline model, precipitation distribution was defined using the National Institute of Water and Atmospheric Research (NIWA) 500 m gridded data [*Tait et al.*, 2006]. Comparison with river flow measurements indicated that the NIWA data are within 25% of the total water input to the catchments in question [*Tait et al.*, 2006], and probably record most rainfall but only some snowfall due to the limitations of standard precipitation gauging techniques [*Goodison*, 1978; *Yang et al.*, 1998]. We applied the method of *Yang et al.* [1998] for a standard rain gauge to estimate the proportion of both precipitation phases that are not recorded by these gauges. The difference in amount between the gauge-estimated values and the modeled precipitation for the model domain was 11% for rainfall and 49% for snowfall, implying that the total annual precipitation amount was 144% of that recorded. To reflect this estimate of gauge undercatch, we increased the precipitation input to the 2-D baseline model by these ratios and again simulated glacier lengths. After increasing precipitation amount in line with this estimate, the LGM Rakaia Glacier simulated under the same ΔT (−6.5°C) was 4.1 km (10%) longer, which equated to a ΔT of less than −0.5°C.

2.3. Experimental Design

Glacier sensitivity to temperature, precipitation amount and distribution, interannual climate variability, temperature seasonality, precipitation seasonality, and precipitation phase was investigated for the eastern Southern Alps. We considered glacier sensitivity to climate change in terms of both change in mass balance and change in glacier length (volume) [cf. *Oerlemans*, 1997]. We performed five sets of experiments, each comprising multiple model simulations, to quantify uncertainty in simulated glacier extents resulting from the following:

1. Experiment 1: Differences in temperature (ΔT) from the baseline model describing present-day climate.
2. Experiment 2: Differences in precipitation amount (P) from the baseline model within a plausible world-wide present-day range.

Table 3. Precipitation Data and the Change in Simulated ELA Resulting From the Use of Different Precipitation Distributions Under Present-Day ($\Delta T = 0$°C) and Double Hill ($\Delta T = -4.5$°C) Scenarios

	Annual Precipitation Within Model Domain (mm)			ELA (m) at	ELA (m) at	ELA (m) Relative to NIWA Results	
Precipitation Data	Maximum	Minimum	Mean (± 1σ)	$\Delta T = 0$°C	$\Delta T = -4.5$°C	$\Delta T = 0$°C	$\Delta T = -4.5$°C
NIWA	8450	645	1602 ± 1129	2201 ± 157	1528 ± 148	0	0
CliFlo	5070	580	2170 ± 1740	2239 ± 202	1650 ± 105	38 ± 180	122 ± 127
Griffiths and McSaveney	8015	868	1512 ± 775	2505 ± 143	1613 ± 113	304 ± 150	85 ± 131
Wratt et al.	5705	444	1134 ± 616	2380 ± 199	1620 ± 117	179 ± 178	92 ± 133
Henderson and Thompson	5373	788	1231 ± 776	2534 ± 108	1682 ± 70	333 ± 133	154 ± 109
Linear function	1769	825	1110 ± 190	2101 ± 102	1419 ± 151	−100 ± 130	−109 ± 150
$NIWA_{mean}$	2141	2141	2141 ± 0	1763 ± 251	1317 ± 137	−438 ± 204	−211 ± 143
$NIWA_{median}$	4854	4854	4854 ± 0	1750 ± 119	1043 ± 173	−451 ± 138	−485 ± 134

3. Experiment 3: Precipitation distribution using five estimated precipitation distributions and three statistical approximations of precipitation for the central Southern Alps (Table 3).
4. Experiment 4: Interannual climate variability defined by the present-day standard deviation of mean melt season (December–February) temperature and annual precipitation amount.
5. Experiment 5: Change in seasonality (*S*), defined here as an increase in monthly summer (October–March) temperatures of up to 3°C, while winter temperatures remain unchanged, combined with change in winter and summer monthly precipitation amounts relative to present-day values.

Despite the possible reduction in LGM precipitation amount of up to 25% indicated by previous glacier modeling [*Golledge et al*., 2012], all experiments used the same values for *P* in the present-day and LGM simulations, apart from those simulations where *P* was explicitly varied. This approach allowed us to isolate the sensitivity to *P* and to compare this directly to differences in temperature and precipitation distribution over a range of climate scenarios. Experiments 1 and 2 tested a range of plausible values of ΔT and *P* during the glacial. Experiments 3 and 5 were designed to simulate specific climate scenarios: (1) the present-day climate applied to the study area by *Rowan et al*. [2013] (Tables 1 and 2); (2) a Late Glacial paleoclimate indicated by the advance of the Rakaia Glacier to produce the Prospect Hill moraine at 16.25 ± 0.34 ka, equivalent to $\Delta T = -3.0$°C [*Putnam et al*., 2013a]; (3) a Late Glacial paleoclimate indicated by the Rakaia Glacier advance to the Double Hill moraine at 16.96 ± 0.37 ka, equivalent to $\Delta T = -4.5$°C [*Putnam et al*., 2013a]; and (4) a paleoclimate representing the LGM at ~21 ka, equivalent to $\Delta T = -6.5$°C [*Golledge et al*., 2012; *Rowan et al*., 2013]. Experiment 4 simulated two scenarios: (1) a Late Glacial advance resulting in a reduction in ELA of ~100 m around ~11 ka [*Kaplan et al*., 2013] equivalent to $\Delta T = -1.25$ °C and (2) the LGM scenario.

Our 2-D glacier model calculated snowfall using the number of days per month for which the daily air temperature in each cell was below a critical value for rain-snow partitioning, using the mean monthly air temperature and its daily standard deviation [*Plummer and Phillips*, 2003]. The value used for the critical temperature at which precipitation falls as snow varies between modeling studies. We tested a range of critical temperatures from 0 to 3°C (results not presented here) which resulted in a 1.9 km (7%) uncertainty in the length of the Pukaki Glacier under present-day climate and a 1.1 km (2%) uncertainty in the glacier length under the Double Hill scenario. The critical temperature was set to 2°C for all simulations reported in this paper. The proportion of annual precipitation falling as snow across the model domain was 7% under the present-day scenario, 46% under the Prospect Hill scenario, 86% under the Double Hill scenario, and 92% under the LGM scenario.

2.3.1. Experiment 1: Temperature

Variations in glacier extent due to ΔT were tested for the Rakaia-Rangitata catchments from −9.0°C to 0°C in 0.5°C increments to find an ELA equivalent to the LGM (799 ± 50 m) and the Prospect Hill advance (1540 ± 50 m). Results are presented in section 3.1.

2.3.2. Experiment 2: Precipitation Amount

P was varied from 25% to 400% of present-day values in 10% or 25% increments to investigate glacier sensitivities in the Rakaia-Rangitata catchments. ELAs were calculated and glacier length simulated under each of the four climate scenarios. Results are presented in sections 3.1 and 3.2. Results from Experiments 1 and 2 (Figure 2) are compared to those produced for the Franz Josef Glacier [*Anderson and Mackintosh*, 2006] and for the Irishman Glacier [*Doughty et al*., 2013].

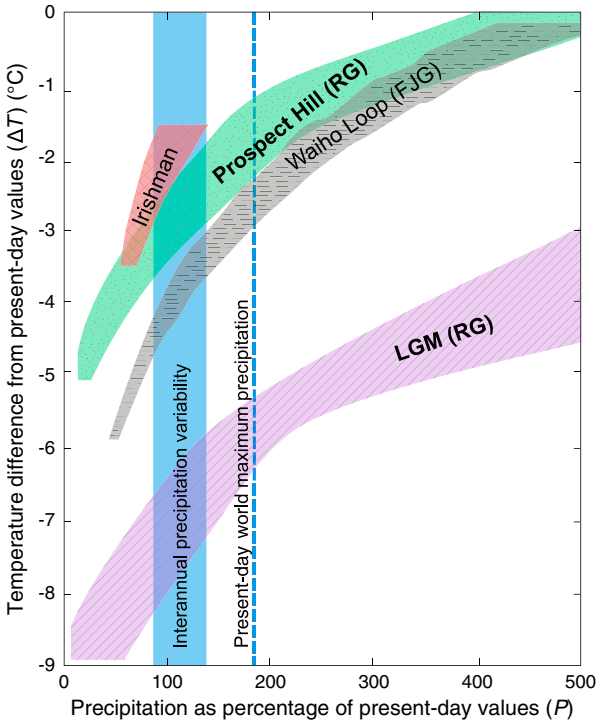

Figure 2. Parameter sets (ΔT and P) for the advance of the Rakaia Glacier (RG) to Prospect Hill (green-dotted shading) and the LGM limit (purple diagonal-hatched shading), compared to results for the advance of the Franz Josef Glacier (FJG) to the Waiho Loop moraine (grey horizontal lined shading) from *Anderson and Mackintosh* [2006], and for the Late Glacial advance of the Irishman Glacier (red cross-hatched shading) from *Doughty et al.* [2013]. The present-day interannual precipitation variability at the FJG (blue shading) and the present-day worldwide precipitation maximum (blue dashed line) are shown [*Henderson and Thompson*, 1999]. As any change in LGM precipitation amount is unlikely to have exceeded the present-day worldwide maximum, the change in climate for these advances probably lies within the blue-shaded area.

2.3.3. Experiment 3: Precipitation Distribution

Orography regulates precipitation distribution over the Southern Alps as the range axis trends perpendicular to the prevailing westerlies. Therefore, the distribution of precipitation is primarily a function of the distance from the west coast of the South Island rather than a function of elevation [*Griffiths and McSaveney*, 1983; *Sinclair et al.*, 1997; *Henderson and Thompson*, 1999; *Ibbitt et al.*, 2001; *Tait et al.*, 2006] (Figures 3b and 3c). When plotted across the range, rain-gauge data show a rather wet region upwind on the western side of the range (3–4 m per year) compared to a much drier region east of the range (less than 2 m per year) (Figure 3a). The scarcity of rain gauges in the high-elevation region 20–60 km downwind of the west coast with which to document this dramatic precipitation gradient leaves open the possibility that glacier simulations could be highly sensitive to the peaks and distribution of precipitation in this region. We assume that precipitation during the LGM was unlikely to have increased beyond the present-day worldwide maximum, equivalent to an 85% increase in Southern Alps precipitation [*Henderson and Thompson*, 1999]. As the last glacial precipitation distribution is unknown, we instead experiment with present-day precipitation distributions for the region and acknowledge that there is unresolved uncertainty when using these to represent last glacial precipitation.

To explore the sensitivity of glacier model results to uncertainty in precipitation distribution, we tested five different estimated present-day precipitation distributions and three statistical approximations of these data for the central Southern Alps: (1–3) three annual rainfall profiles [*Griffiths and McSaveney*, 1983; *Wratt et al.*, 1996; *Henderson and Thompson*, 1999]; (4) gridded 500 m monthly NIWA rainfall data [*Tait et al.*, 2006]; and (5) rain-gauge data from the CliFlo database fitted with a least squares cubic spline approximation that preserves shape. Based on these rainfall data, we tested three statistical approximations of precipitation distribution; (6) a linear relationship linking rainfall to elevation derived from regression of the CliFlo data, and grids of (7) median, and (8) mean monthly values derived from the NIWA data. Where rainfall data provided only annual values, these were divided into monthly totals using the present-day distribution in the NIWA data. These 1-D profiles represent rainfall along a section oriented at 130° through the center of the model domain (Figure 1a). A mean topographic profile defined from a 40 km wide swath centered on this transect (Figure 3) was used to interpolate the linear precipitation values in test (6). The rainfall data were converted to 2-D grids by duplicating these profiles along strike of the range axis perpendicular to the transect. The mean annual precipitation amount varied with the choice of precipitation distribution. For the distributions in tests (1) to (4), mean annual precipitation across the model domain varied between the different data sets from 1134 to 1602 mm (Table 3). Results are presented in section 3.3.

2.3.4. Experiment 4: Interannual Climate Variability

Interannual variability in mean melt season temperature and annual precipitation amount (often described as white noise) can cause kilometer-scale fluctuations in glacier length independent of climate change

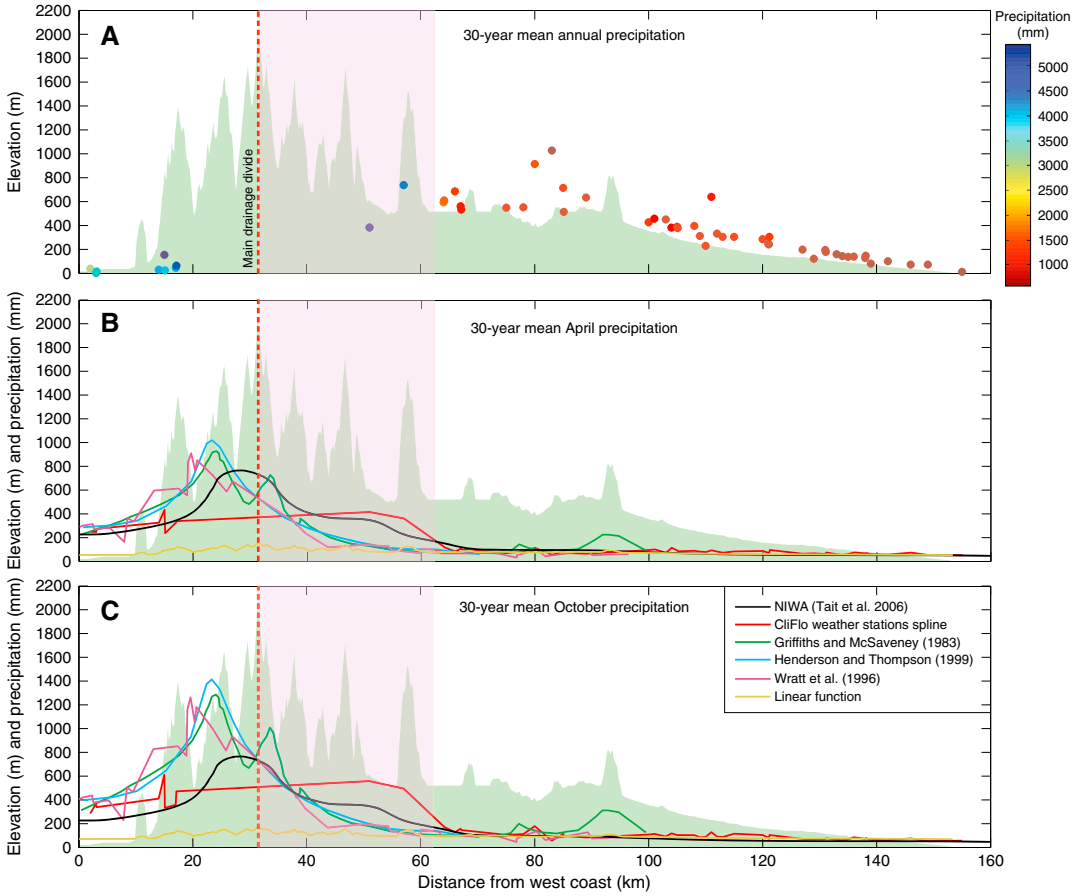

Figure 3. Precipitation amount along a 1-D transect through the center of the model domain orientated at 130°. (a) Annual 30 year mean precipitation data collected from rain gauges within 50 km of the transect (filled points), 30 year monthly mean precipitation amount for (b) April and (c) October, showing 1-D precipitation profiles for central Southern Alps [*Griffiths and McSaveney*, 1983; *Wratt et al*., 1996, 2000; *Henderson and Thompson*, 1999; *Tait et al*., 2006], CliFlo rain gauge data fitted with a least squares cubic spline that preserves shape, and a linear function linking rainfall to elevation derived from the CliFlo data. The mean topographic profile of the model domain (green shading), the position of the main drainage divide (red dashed line), and the 30 km region downwind of the main drainage divide where glacier sensitivity to precipitation amount is greatest (pink shading) are shown. Note that some points in Figure 3a occur above the mean topographic profile as the stations are located above the mean elevation along this transect. Also note the different units for elevation (m) and precipitation (mm) on the *y* axis of Figures 3b and 3c.

[e.g., *Oerlemans*, 2001; *Roe and O'Neal*, 2009; *Roe*, 2011]. These fluctuations add a one-sided bias to paleoclimate estimates derived from the moraine record, as the terminal moraine position for a particular advance represents the maximum down-valley excursion of the glacier rather than the mean glacier length [*Anderson et al*., 2014]. We used a 1-D flowline model with variable width to determine the mean length for the Late Glacial ($\Delta T = -1.25$°C) and LGM ($\Delta T = -6.5$°C) Rakaia Glacier. To maintain coherence between our glacier models, mass balance calculations produced using the 2-D model were used to describe the 1-D mass balance profiles for this glacier. The advantage of using a 1-D model to test sensitivity to interannual climate variability is that we can efficiently run hundreds of simulations with independent white-noise realizations, therefore allowing us to establish the most probable mean glacier length for a particular advance.

Two independent white-noise realizations for mean melt-season temperature and annual precipitation amount were used for each simulation. The temperature realization was modified by a random normal distribution of annual values using the standard deviation of mean December–February temperature (0.8°C) from the Lake Coleridge AWS (Figure 1). The annual precipitation realizations were modified by a random normal distribution of annual values using the standard deviation of precipitation data from AWS on the west side of the range (870 mm per year). Data derived from AWS in the eastern Southern Alps do not capture the

precipitation variability in present-day glacier accumulation areas (Figure 3) [*Woo and Fitzharris*, 1992]. However, the *Woo and Fitzharris* [1992] data provide a minimum estimate of the annual precipitation variability in the glacier accumulation areas, because these data are derived from a low-elevation AWS and neglect the effects of wind-blown snow and avalanching. Mass balance was perturbed from a mean state using a melt factor of 0.9 m water equivalent per °C per year; a representative value based on a global compilation of present-day melt factors for ice [*Anderson et al*., 2014]. Results are presented in section 3.4.

2.3.5. Experiment 5: Seasonality

The range of monthly mean summer and winter temperatures and precipitation amounts are likely to change during a glacial [*Nelson et al*., 2000; *Golledge and Hubbard*, 2009]. Sea surface temperature records for the LGM indicate that temperature seasonality (*S*) was 3°C in Canterbury Bight [*Nelson et al*., 2000; *Drost et al*., 2007] and 2°C across the region [*Barrows and Juggins*, 2005]. Previous LGM regional climate modeling indicated *S* equivalent to an increase in summer temperatures of 0.7°C in eastern South Island, lower than the mean value of 1.1°C for New Zealand, and summer precipitation slightly higher and winter precipitation slightly lower than present-day values [*Drost et al*., 2007]. To quantify how a realistic variation in *S* from present-day values affects ELA, we compared glaciers simulated with the baseline model to simulations using an estimated maximum LGM seasonality of the following:

1. Summer temperature (October–March) = Present-day temperature + 3°C
2. Summer precipitation (October–March) = Present-day precipitation * 1.11
3. Winter temperature (April–September) = Present-day temperature
4. Winter precipitation (April–September) = Present-day precipitation * 0.97

These values for *S* follow the results of regional meteorological modeling of the LGM in New Zealand by *Drost et al*. [2007]. Results are presented in section 3.5.

3. Results

The variability in simulated glacier lengths and ELAs resulting from sensitivities to difference in temperature, precipitation amount, precipitation distribution, interannual climate variability, and seasonality are presented here. Transient ice flow calculations show that steady state was reached within 400 years for $\Delta T = 0.5$°C, consistent with the response times of up to hundreds of years estimated using analytical solutions [*Jóhannesson et al*., 1989]. Response time for the present-day Tasman Glacier in the Pukaki valley was estimated as 20–200 years by assuming terminus ice thickness of ~500 m and an ablation rate beneath the thick debris layer of 2.5 m per year. The range of values indicates the potentially large uncertainty in predictions of melt rates beneath supraglacial debris [*Herman et al*., 2011].

3.1. Experiment 1: Glacier Sensitivity to Change in Temperature and Precipitation

Present-day and LGM ELAs simulated using the 2-D glacier model were compared to ELAs reconstructed using the accumulation-area ratio method (with a value for the ratio of the accumulation area to the total glacier area of 0.6 ± 0.05) for the Pukaki and Tekapo valleys [*Porter*, 1975]. The parameter space required to produce LGM and Prospect Hill ELAs was tested for the Rakaia-Rangitata catchment and compared to previous estimates for the Franz Josef Glacier [*Anderson and Mackintosh*, 2006] and the Irishman Glacier [*Doughty et al*., 2013]. We tested ΔT and *P* values to produce ELAs required to advance glaciers to the LGM and Prospect Hill terminal moraines. *P* was limited within a realistic range for the present-day interannual variability in the Southern Alps (80–140% of present-day values) and up to the present-day worldwide maximum (185%) [*Henderson and Thompson*, 1999].

LGM ELAs were simulated under conditions where $\Delta T = -8.0$°C to -5.5°C and $P = 80\%$ to 175% of present-day values. If change in precipitation amounts were restricted to the range of regional interannual variability, the LGM would have occurred with ΔT of -8.25°C to -6.0°C. We assume little or no change in precipitation amount during the LGM, to give solutions of $\Delta T = -6.5$°C and $P = 100\%$ for the LGM and $\Delta T = -3.0$°C and $P = 100\%$ for the Prospect Hill advance [*Putnam et al*., 2013a]. The sensitivity of glacier extent to ΔT was tested for the Rakaia and Rangitata Glaciers and varied with the absolute value of ΔT (Figure 4). The length of the Rakaia Glacier increased by at least 37% with $\Delta T = 0.5$°C when the absolute value of ΔT was minimal (less than -2.0°C) compared to present-day conditions. The relative change in glacier length decreased with moderate differences in temperature ($\Delta T = -3.5$°C to 5.0°C) to 8%, then increased with greater absolute differences in

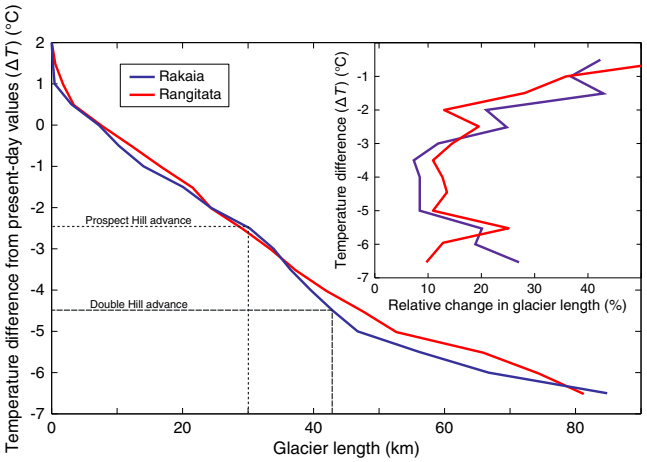

Figure 4. Change in length of Rakaia and Rangitata Glaciers with ΔT. Inset shows the relative change in glacier length as a percentage of the total LGM glacier length. The location of Prospect Hill and Double Hill are noted.

temperature ($\Delta T = -5.5$°C to -6.5°C) to ~23%. A similar trend was found for the Rangitata Glacier (Figure 4), and the decrease in glacier length change occurs when the glaciers extend into the trunk valleys where bed slopes are lower. Under the LGM scenario, $\Delta T = -1$°C increased the length of the Rakaia Glacier by 28.7 km (51%).

3.2. Experiment 2: Glacier Sensitivity to Precipitation Amount

Glacier sensitivity to precipitation amount was tested for the Rakaia Glacier by varying P from half to twice the present-day values under present-day, Double Hill, and LGM scenarios (Table 4). This range of P values tested exceeds the present-day interannual variability of precipitation amount in the Southern Alps. Under present-day conditions, halving P produced no glacier ice at the headwall of the Rakaia Glacier and reduced the length of the Pukaki Glacier by 13.4 km (-51%). A 50% increase in P increased the length of the Rakaia Glacier by 2.2 km (78%) and the Pukaki Glacier by 3.7 km (14%). Doubling P increased the length of the Rakaia Glacier by 5.7 km (203%) and the Pukaki Glacier by 13.9 km (53%). Under Double Hill conditions, halving P reduced the length of the Rakaia Glacier by 6.6 km (-18%) and reduced the length of the Pukaki Glacier by 10.2 km (-14%), whereas a 50% increase in P increased the length of the Rakaia Glacier by 3.1 km (9%) and the Pukaki Glacier by 3.5 km (5%). The experiment under Double Hill conditions where P was doubled did not reach a stable solution due to an unrealistically positive mass balance. Under LGM conditions, a 25% increase in P produced the equivalent increase in length of the Rakaia Glacier to $\Delta T = -0.5$°C. Sensitivity to P was lower for the Double Hill simulations, requiring a greater increase ($P = 150$% rather than 125%) to produce the change in glacier extent resulting from $\Delta T = -0.5$°C (Figure 2). For the LGM scenario, glacier sensitivity to ΔT decreases as P exceeds the present-day worldwide maximum; if P was double the present-day value, ΔT of -0.5°C would be equivalent to an increase in P of 50%, indicating that P modifies the temperature sensitivity of these glaciers.

Table 4. Comparison of the Change in Length of the Simulated Pukaki and Rakaia Glaciers Resulting From Experiments Testing Temperature, Precipitation Amount, and Precipitation Distribution Under Present-Day ($\Delta T = 0$°C) and Double Hill ($\Delta T = -4.5$°C) Scenarios[a]

		Present-Day ($\Delta T = 0$°C)		Double Hill ($\Delta T = -4.5$°C)	
Experiment	Variable	Pukaki Glacier Length (km)	Rakaia Glacier Length (km)	Pukaki Glacier Length (km)	Rakaia Glacier Length (km)
1. Temperature difference	ΔT, $P = 1$	26.2	2.8	71.8	36.6
2. Precipitation amount	$P = 0.5$	12.8	0.0	61.6	30.0
	$P = 1.5$	29.9	5.0	75.3	39.7
	$P = 2.0$	40.1	8.5	[b]	[b]
3. Precipitation distribution	CliFlo automatic weather stations	13.6	0.0[a]	60.9	31.5
	Griffiths and McSaveney [1983]	1.0	0.0[a]	54.7	25.7
	Henderson and Thompson [1999]	1.7	0.0[a]	54.7	27.3
	Wratt et al. [1996]	14.3	0.0[a]	59.9	30.3

[a]The Rakaia Glacier length is zero in some present-day simulations as no ice is present at the headwall of this catchment. In Experiments 1 and 2, the precipitation data used are the NIWA grids.
[b]The solution for the simulation where precipitation was doubled under the Double Hill scenario did not reach steady state due to an unrealistically high mass balance—these results are not presented.

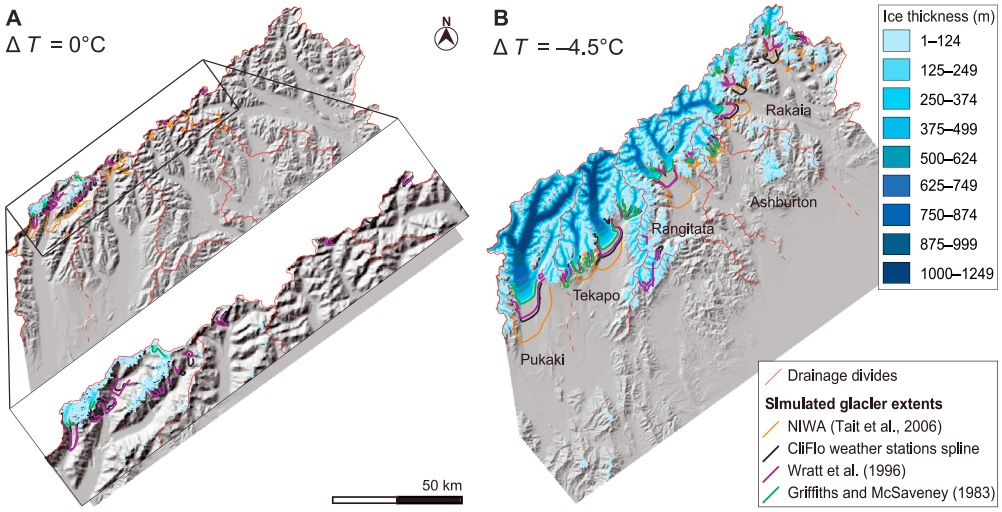

Figure 5. Glaciers simulated using five different precipitation distributions under (a) the present-day ($\Delta T = 0$°C) and (b) the Double Hill ($\Delta T = -4.5$°C) scenarios. The blue shading shows glaciers simulated using the *Henderson and Thompson* [1999] profile. The glaciers simulated using the NIWA precipitation data [*Tait et al.*, 2006] (orange lines), CliFlo (black lines), *Wratt et al.* [1996] (purple lines), and *Griffiths and McSaveney* [1983] (green lines) profiles for the same climate scenarios are also shown. Inset to Figure 5a shows the glaciated area at the main drainage divide in detail.

3.3. Experiment 3: Glacier Sensitivity to Precipitation Distribution

The choice of precipitation distribution had a considerable influence on the extent of the simulated glaciers (Figure 5 and Table 4) and the regional ELA (Table 3). The precipitation peak in each profile is located upwind of the main drainage divide and precipitation amounts are similar downwind of 70 km from the west coast (Figure 3), suggesting that glaciers are sensitive to the volume of precipitation delivered within the zone up to 30 km downwind of the main drainage divide (32 km from the west coast; Figure 3). Under both present-day and Double Hill conditions, glacier extents simulated using published precipitation distribution profiles were greatest when using the NIWA data, followed by the CliFlo, then *Wratt et al.* [1996] profiles, and least with the *Griffiths and McSaveney* [1983] and *Henderson and Thompson* [1999] profiles (Figure 5 and Table 4). The change in ELA using published precipitation distribution profiles relative to the NIWA results was greatest with the *Henderson and Thompson* [1999] data; ELA change of 333 m under present-day conditions and 154 m under the Double Hill scenario (Table 3). Across the range of precipitation distributions tested, the variation in glacier length under present-day conditions was 24.5 km (93.5%) for the Pukaki Glacier and 2.8 km (100%) for the Rakaia Glacier. Under Double Hill conditions, the variation in length was less for the Pukaki Glacier (17.1 km; 24%) and greater for the Rakaia Glacier (9.3 km; 25%) compared to present-day conditions although the absence of ice in four of the present-day Rakaia simulations affected this result (Table 4).

Results produced using mean and median precipitation distributions show that, although the maximum precipitation amount for these experiments was less than that in the NIWA gridded data, ELAs were lower (−438 m and −451 m) as the value for the minimum precipitation amount was greater than that from the NIWA data. Change in ELA due to precipitation distribution was greatest under present-day climate conditions (191 m) compared to the Double Hill advance (91 m) (Table 3). The linear regression of precipitation measurements gave the lowest value for total precipitation amount and produced an ELA ~100 m lower than those simulated using the NIWA data for the present-day and Double Hill scenarios (Table 3). Under LGM conditions, glacier extents calculated using the linear regression were similar to those produced under Double Hill conditions using the NIWA data, equivalent to $\Delta T = 2$°C. If we exclude those glaciers simulated using statistical approximations of precipitation distribution and consider only the glaciers simulated using the five estimated rainfall distributions, then the change in ELA due to precipitation distribution was 171 m under present-day conditions and 91 m for the Double Hill scenario. Of the variables tested in our experiments, after difference in temperature, glaciers were most sensitive to precipitation distribution.

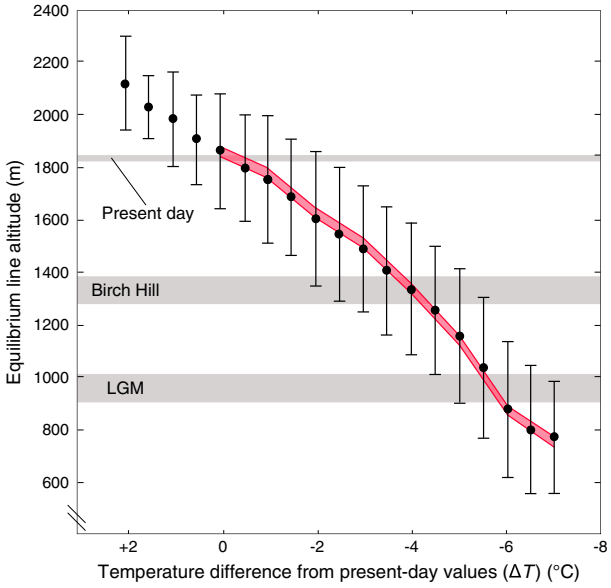

Figure 6. Change in ELA with ΔT for the Rakaia-Rangitata domain (black points) with 1 standard deviation uncertainty compared to ELAs reconstructed for the eastern Southern Alps [*Porter*, 1975], and variations in ELA resulting from an estimated maximum LGM seasonality (red bar).

3.4. Experiment 4: Glacier Sensitivity to Interannual Climate Variability

We tested the effect of interannual climate variability on glacier length using a 1-D model of the Late Glacial ($\Delta T = -1.25$°C; ~12 km long glacier) and LGM ($\Delta T = -6.5$°C; ~80 km long glacier) advances of the Rakaia Glacier. The Late Glacial glacier was formed by three tributaries converging within 3 km of the maximum glacier extent. To capture this complex glacier geometry, we modeled all three tributary glaciers and fed the two smaller tributaries into the larger trunk glacier. As a result, these simulations consider the terminus fluctuations resulting from the independent response of each of the three tributary glaciers [cf. *MacGregor et al.*, 2000; *Zuo and Oerlemans*, 1997]. We compared glacier extents simulated using the 1-D model to those from 2-D simulations; a 1.25°C increase in mean summer temperature produced a 5 km recession from the Late Glacial maximum that is similar to the difference in extent between the Late Glacial and present-day glaciers, demonstrating that our 1-D model is reasonably sensitive to summer temperature perturbations in comparison to the 2-D model.

Each Late Glacial simulation ran for 1000 years [e.g., *Kaplan et al.*, 2010]. One thousand simulations were used to estimate the most probable mean glacier length for the Late Glacial advance, which was ~1300 m shorter (10% of the maximum glacier length; equivalent to $\Delta T = +0.2$°C) than the terminal moraine. The standard deviation of the mean length from the most likely mean length was 560 m, and the standard deviation of glacier length was 825 m. These results imply that paleoclimate estimates from the Late Glacial terminal moraine position will overestimate the mean glacier length by 10%. This variability accounts for 26% of the change in length required to advance from the present-day position to the Late Glacial terminus. The standard deviation of the modeled snowline elevation was 110 m, which is within the window of present-day snowline variability in New Zealand [*World Glacier Monitoring Service* (*WGMS*), 2013]. The standard deviation of net mass balance, summer balance, and winter balance were 1.15 m, 0.9 m, and 0.7 m per year. These simulated values are similar to mass balance measurements made for the Ivory Glacier (~15 km to the north of the Rakaia) where the standard deviation of annual mean mass balance, summer balance, and winter balance were 1.1 m, 0.63 m, and 0.87 m per year between 1970 and 1975 [*WGMS*, 2013].

Each LGM simulation ran for 4000 years. One hundred simulations were used to estimate that the most probable LGM mean glacier length was 2.3 km shorter (2.8% of the maximum glacier length; equivalent to $\Delta T = +0.1$°C) than the terminal moraine defined by *Shulmeister et al.* [2010]. The standard deviation of the mean length from the most likely mean length was 840 m, and the standard deviation of the glacier length was 1200 m. These results imply that paleoclimate estimates using the LGM terminal moraine position will overestimate the mean glacier length by 2.8%. The standard deviation of the modeled snowline elevation was 100 m. The standard deviation of annual mean mass balance, summer balance, and winter balance were 1.09 m, 0.72 m, and 0.82 m per year.

3.5. Experiment 5: Glacier Sensitivity to Seasonality

Glacier sensitivity to S was tested for ΔT from 0°C to −7°C using the maximum estimated LGM seasonality (Figure 6). Under present-day conditions, the ELA was reduced by just 3 m due to S. ELA change due to S was greatest when glaciers were less extensive but did not exceed 41 m across the range of ΔT values tested. LGM ELAs were 13 m lower due to changes in S than those for the same climate scenario using present-day values

for seasonality. In comparison, ΔT of −1°C under the LGM scenario resulted in a decrease in ELA of 146 m—much greater than that due to changes in *S* (Figure 6). Glacier sensitivity to seasonality was not sufficient to be resolved beyond the model uncertainty, and our results indicate the limitations of glacier modeling as a means of reconstructing the finer details of LGM paleoclimates from the geological record.

3.6. Summary of Results

Glaciers were sensitive to differences in mean annual air temperature (ΔT), the distribution of precipitation, and precipitation amount (*P*) (Table 4). Glacier sensitivity to seasonality in temperature and precipitation amount and to interannual climate variability was within the uncertainty ascribed to the climatological parameter values used in our simulations. Based on our results and previous testing of the uncertainty associated with the model parameter values by *Plummer and Phillips* [2003], we consider the minimum ΔT value that can be resolved to be 0.25°C. Therefore, we consider only those variations in simulated glacier length that exceed those produced by $\Delta T = 0.25$°C to indicate significant climate sensitivity. For the Rakaia Glacier under present-day conditions, the change in glacier length indicating significant climate sensitivity is 1.9 km (13%). Under the Double Hill scenario this value is 3.0 km (15%). Under the LGM scenario this is 4.7 km (12%).

The percentage change in glacier length varied with the magnitude of ΔT. Glacier length percentage change from the present-day extent was least under intermediate differences in temperature ($\Delta T = -3.5$°C to 5.0°C). Glacier length change per degree ΔT was greatest when glaciers were very small or very large (approaching their LGM limits) (Figure 4). Small glaciers advanced more rapidly with relatively small changes in mass balance, and they advanced at a faster rate as tributary glaciers merged into the main valley glaciers. ΔT of 0.5°C offset values of *P* within the present-day worldwide range [*Henderson and Thompson*, 1999], indicating that change in LGM precipitation amount had a minor effect on glacier extents in the Southern Alps in comparison to difference in temperature.

Glaciers were sensitive to change in precipitation distribution, with change in glacier length of 25% occurring across the range of precipitation distributions tested under the Double Hill scenario, equivalent to ΔT of at least 0.5°C. If a linear regression linking precipitation distribution to the topographic surface based on measurements from AWS was used instead, then the offset in simulated mass balance for LGM conditions was equivalent to ΔT of 2°C. Using uniform precipitation distributions with values taken from the mean and median of regional values gave unrealistic mass balance for each climate scenario, with ELA depressions of ~400 m relative to using the NIWA data. Glacier sensitivity to precipitation distribution was greatest within 30 km downwind of the main drainage divide where the largest accumulation areas occur, and sensitivity to both precipitation amount and distribution decreased with increasing cooling (increased ΔT). Using our definition of model resolution ($\Delta T = 0.25$°C), the importance of variations in glacier length produced by *P* decreased with increased ΔT, but the variation in glacier length produced using a range of plausible present-day precipitation distributions remained significant across all of our climate scenarios.

4. Discussion

The use of glacier models to estimate paleoclimate requires assumptions about a number of climatological and glaciological parameters. In this paper, we explored glacier sensitivity to paleoclimate variables by comparing the glacier volumes simulated with a realistic range of values for difference in temperature, precipitation amount, precipitation distribution, interannual climate variability, and seasonality. Here we discuss the implications of these sensitivities for the reconstruction of LGM glaciers in the Southern Alps. The Rakaia Glacier, which has proved particularly challenging in previous modeling studies, is discussed in detail. We also discuss further sources of uncertainty that should be considered in the application of glacier models—factors that influence mass balance such as radiative fluxes and avalanching, the representation of topography, and the choice of model domain and grid spacing.

4.1. LGM Climate Variability in the Southern Alps

ELA sensitivity to ΔT and *P* for the Rakaia-Rangitata Glaciers show a similar relationship to those calculated for the Franz Josef Glacier [*Anderson and Mackintosh*, 2006]. Our present-day climate simulations gave an ELA for the Pukaki and Tekapo valleys similar to those reconstructed by *Porter* [1975] (Figure 6). Our LGM simulations produced an ELA slightly lower than those estimated for the Pukaki and Tekapo Glaciers although the value is within the uncertainty window stated by *Porter* [1975]. The gradient of simulated ELA

along the eastern side of the range indicated that slightly greater cooling was needed to simulate glaciers that extended to the LGM moraines further north. ΔT of -4.5°C forced the advance of the Rakaia Glacier to Double Hill at ~17 ka [*Putnam et al*., 2013a] for which there is no equivalent advance identified elsewhere in the Southern Alps. ΔT of -4.5°C also forced the advance of the Pukaki Glacier to the Birch Hill moraines at ~13 ka [*Putnam et al*., 2010], and a similar ΔT of -4.0°C forced the advance of the Franz Josef Glacier to the Waiho Loop moraine at ~13 ka [*Anderson and Mackintosh*, 2006], although the climatic significance of this advance is unclear [e.g., *Tovar et al*., 2008]. The cooling required for simulated glaciers to reach LGM extents ($\Delta T = -6.5$°C) is in agreement with the 4–7°C of cooling estimated from LGM sea surface temperatures [*Barrows et al*., 2007; *Bostock et al*., 2013] and previous regional glacier modeling [*Golledge et al*., 2012].

4.2. The Rakaia Glacier

Golledge et al. [2012] identified those glaciers with large overdeepenings farthest from their accumulation areas, including the Rakaia, as those most challenging to model reconstructions; to obtain a successful simulation of the Rakaia Glacier, temperature for the entire Southern Alps icefield was -1.5°C to -2.0°C below that used for the LGM in other eastern valleys [*Golledge et al*., 2012]. Such large uncertainties may be attributed to (1) catchment-scale meteorological variability forced by orography and therefore not represented in regional climate data, (2) the limitations of the approximations used in glacier modeling that do not completely conserve mass, or (3) the composition of the bed and its influence on subglacial motion. Finer-resolution (200 m compared to 500 m grid spacing) simulations for the Rakaia-Rangitata Glaciers [*Rowan et al*., 2013] reached an improved solution which showed a greater degree of synchroneity between these glaciers but still had a ΔT of -0.25°C between the LGM extent of the Rakaia and that of both the neighboring Rangitata and Ashburton Glaciers.

4.3. Uncertainty due to the Description of Mass Balance

Many glacier models use empirically-derived accumulation and ablation rates measured in the field or based on relevant degree-day factors to describe mass balance [*Braithwaite*, 1995; *Hock*, 2003]. However, the assumption of a linear relationship between mass balance and elevation may be inaccurate because steep topography modifies radiative energy fluxes and the redistribution of snow by avalanching. We instead used a 2-D energy balance calculation based on a monthly climatology derived from local AWS and incorporated the effects of topographic shading and avalanching into the calculation of mass balance [*Plummer and Phillips*, 2003]. Using 2-D meteorological data allows the investigation of glacier sensitivity to spatial variability in mass balance which is not considered in 1-D models. This paper uses present-day 30 year mean meteorological data to capture the regional orographic trend in precipitation distribution (Figure 3). However, precipitation may exhibit a more complex distribution than can be captured at the resolution of these gridded data (the NIWA data have a grid spacing of ~4 km), and catchment-scale variations may be unaccounted for in regional gridded precipitation data.

4.4. Uncertainty due to Interannual Variability

The position of a glacier terminus can fluctuate even in the absence of a change in climate. Variations in mass balance forced by interannual climate variability can produce nested sets of moraines. For a given advance, the outermost terminal moraine will therefore represent the maximum rather than the mean glacier length [*Anderson et al*., 2014]. While the magnitude of the most likely maximum fluctuation of the Rakaia Glacier was larger for the LGM than for the Late Glacial (2.3 km compared to 1.3 km), the LGM fluctuations represent a smaller percentage of the maximum glacier length (2.8% compared to 10%). Ice extents preserved within 2.8% and 10% of the terminal moraine position for the LGM and Late Glacial advances could therefore be explained by climate noise rather than climate change.

The standard deviation of annual precipitation amount ($\sigma_P = 0.9$ m per year) and summer temperature ($\sigma_T = 0.8$°C) for the Southern Alps are comparable to those for other maritime regions. For example, $\sigma_P = 1.0$ m per year and $\sigma_T = 0.8$°C in the North Cascade Mountains, USA [*Roe and O'Neal*, 2009]; $\sigma_P = 0.9$ m per year and $\sigma_T = 0.7$°C at Nigardsbreen in Norway (G.H. Roe and M.B. Baker, submitted to *Journal of Glaciology*, 2014), and an exceptional case with a continental climate of $\sigma_P = 0.22$ m per year and $\sigma_T = 1.3$°C for the Colorado Front Range, USA [*Anderson et al*., 2014]. The standard deviations of the length of the simulated Rakaia Glacier (850 m and 1200 m) are large compared to those for other simulated glaciers forced by interannual variability. For example, 180 m for the Rhonegletscher and 360 m for Nigardsbreen [*Reichert et al*., 2002]; 415 m for the

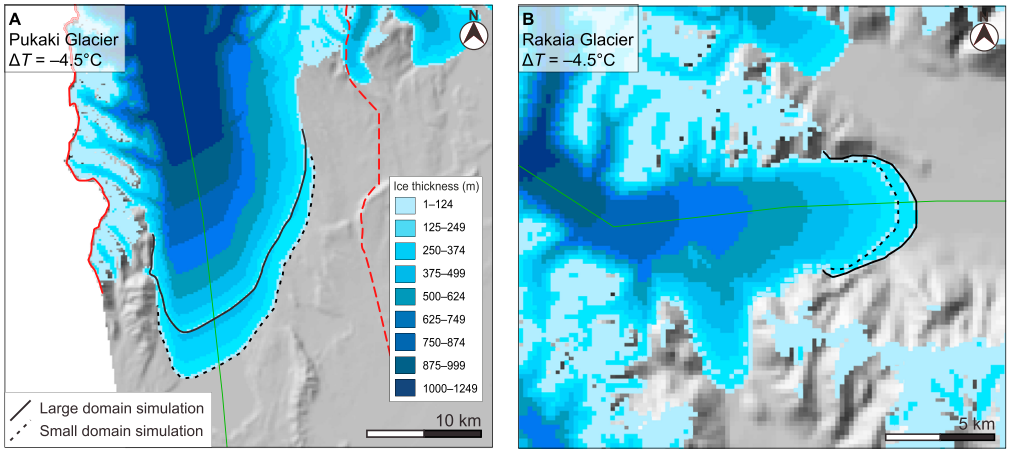

Figure 7. Double Hill ($\Delta T = -4.5$°C) simulations for the (a) Pukaki and (b) Rakaia Glaciers. In each case, ice extent and terminus position are shown for the simulation using the model domain including the Pukaki, Tekapo, and Rakaia-Rangitata catchments (solid black line). Terminus position for the simulations applied to a smaller domain covering just the catchment in question (dashed black lines) and flowlines used to measure glacier length (green solid lines) are also shown.

North Cascades, USA [*Roe and O'Neal*, 2009]; and 280–960 m for the Colorado Front Range [*Anderson et al.*, 2014]. The large standard deviations of the length of the Rakaia Glacier are the result of the large variability in annual precipitation and mean melt-season temperature typical of maritime climates.

Our results imply that interannual climate variability may significantly affect advances that are less than or as extensive as the Late Glacial Rakaia advance. Future modeling studies should consider that smaller advances could be explained by climate noise without implicating changes in climate. The magnitude of the standard deviations of the length of the Late Glacial and LGM advances is amplified by the low bed slopes of these glaciers (~5% slope for the Late Glacial and ~0.5% slope for the LGM Rakaia), as large glacier area relative to the ablation zone slopes enhances length fluctuations due to climate noise [*Roe and O'Neal*, 2009, equation 11]. The uncertainties in the 2-D mass balance model inputs overwhelm the effect of interannual climate variability on paleoclimate estimates for the Late Glacial and LGM Rakaia advances. However, the nearest present-day glacier to the Late Glacial extent is ~5 km upvalley, and interannual variability could have forced an advance accounting for up to 26% of the total Late Glacial advance from the present-day glacier position. Furthermore, current New Zealand meteorological records do not cover a long enough time span to confidently test for conditional probability in the climate system [e.g., *Burke and Roe*, 2013], which could greatly enhance the magnitude of interannual climate variability forced advances.

4.5. Uncertainty due to the Choice of Model Domain and Grid Spacing

Adjacent glaciers may not reach steady state synchronously [*Oerlemans et al.*, 1998]. The simulations presented in our study were performed over the model domain composed of three major catchments—the Pukaki, Tekapo, and Rakaia-Rangitata (Figure 1). We compared steady state ice volumes between two domains with the same grid spacing (200 m) but with different grid extents. We applied identical simulations for present-day and Double Hill scenarios to the entire model domain and to subdomains representing just the Pukaki or Rakaia-Rangitata catchments. Under present-day conditions ($\Delta T = 0$°C), there was no difference in simulated glacier extents between domains. However, under the Double Hill scenario ($\Delta T = -4.5$°C), the Rakaia Glacier was 0.81 km (2%) shorter and the Pukaki Glacier was 4.3 km (6%) longer for the small domain simulations compared to those for the large domain (Figure 7).

The conservation of ice mass was monitored in each simulation, as spurious output may result when the calculated flux from a cell is greater than the ice mass in that cell [*Jarosch et al.*, 2013]. Mass conservation was improved for simulations with a smaller grid spacing (100 m compared to 200 m). However, there is a tension in the choice of grid spacing, as halving this value quadruples the number of cells in the model domain, and computation time increases exponentially. We compared identical simulations with different grid spacings to calculate the change in simulated length of the Rakaia Glacier. As the 100 m grid spacing simulations were more computationally expensive to run, we only tested small values for ΔT. Compared to the 200 m grid

spacing; with $\Delta T = -1.0$°C a 100 m grid spacing produced a glacier 0.7 km (6%) shorter; and with $\Delta T = -2.25$°C equivalent to the Reischek Knob 1 advance [*Putnam et al*., 2013a] a 100 m grid spacing produced a glacier 0.8 km (3%) shorter. Conservation of mass was improved by an order of magnitude using a 100 m grid spacing, from an integrated mass balance of between −5% and −1% to less than −0.5%. Simulations with a smaller grid spacing resulted in a systematically slightly less-extensive glacier than those with a coarser grid.

The variations in glacier length resulting from the use of different model domains and either a 200 m or 100 m grid spacing is equivalent to $\Delta T < 0.1$°C which is smaller than the uncertainty ascribed to the application of the glacier model (equivalent to change in glacier length of 13% and $\Delta T = 0.25$°C). Within the range of values tested, the size of the model domain and the grid spacing are not considered to represent a significant source of uncertainty, and the larger grid spacing is preferable to allow less expensive computation. Conservation of mass improved as ΔT increased; integrated glacier balance was no greater than −2% when ΔT exceeded −5°C, indicating that this uncertainty is relatively small for larger glaciers.

5. Conclusions

The sensitivity of glaciers in the Southern Alps of New Zealand to mean annual air temperature, precipitation amount, precipitation distribution, interannual climate variability, and seasonality was tested using two glacier models. Variations in mass balance and glacier length were governed primarily by differences in mean annual air temperature and the distribution of precipitation. The variations in glacier lengths resulting from the choice of precipitation data were equivalent to those resulting from a difference in temperature of 0.5°C. However, if precipitation were calculated as a function of elevation, a larger uncertainty in the simulated glacier length would be produced, equivalent to a difference in temperature of 2°C. Interannual climate variability and seasonality added relatively minor uncertainties to our paleoclimate estimates, although the effect of interannual variability was important for advances comparable to or smaller than that during the Late Glacial extent at ~11 ka.

Within a plausible range of precipitation variability for the Southern Alps (80–140% of present-day regional values), the Last Glacial Maximum (LGM) occurred with a difference in temperature from present-day values of −8.25°C to −6.0°C, or up to −5.5°C if the present-day worldwide maximum precipitation amount (175%) was used. This LGM paleoclimate envelope captures the possible climatic variability indicated by the glacial geological record, based on the assumption that precipitation during the glacial was in the present-day worldwide range, and includes the ±0.25°C uncertainty assigned to the choice of precipitation data. To account for the total uncertainty in the LGM simulations resulting from other climatological variables (the critical temperature for rain-snow partitioning, interannual variability, and seasonality), we assign an additional uncertainty of ±0.25°C.

Glacier models require a spatial representation of precipitation, the distribution of which is difficult to quantify even under present-day conditions. Rainfall data are collected at a relatively large number of weather stations in the Southern Alps and some snowfall measurements are also made, but estimates of orographic precipitation distributions still contain substantial uncertainties. Our results demonstrate the importance of quantifying sensitivity to a range of precipitation distributions when making glacier model reconstructions, and of considering the uncertainty resulting from how precipitation distribution may have varied from present-day values during the last glacial. Future glacier modeling studies should test a range of plausible precipitation distributions to quantify these uncertainties rather than relying on empirical relationships between precipitation amount and elevation. Without these data describing precipitation distribution, we expect the resolution of our Southern Alps glacier model to be ±0.5°C. However, by testing a range of precipitation distributions, we can estimate the paleoclimate envelope represented by a particular set of moraines and can resolve past differences in temperature greater than ±0.25°C from the late Quaternary moraine record.

Acknowledgments

A.V. Rowan was supported by a post-doctoral fellowship from the Climate Change Consortium of Wales (C3W), and some of this research was carried out under Natural Environment Research Council (NERC) studentship NE/F008295/1. S.H. Brocklehurst is partially supported by a University of Canterbury Visiting Erskine Fellowship. D.M. Schultz is partially supported by NERC grant NE/I026545/1 Precipitation Structures over Orography (PRESTO). L.S. Anderson is supported by National Science Foundation grant DGE-1144083 (GRFP). The National Institute of Water and Atmospheric Research (NIWA) Ltd. provided the gridded rainfall data used in some simulations. Land Information New Zealand (LINZ) provided the digital elevation model. Gerard Roe is thanked for his comments on the white noise experiments. We thank the Editor Alex Densmore and the Associate Editor Mike Bentley for their helpful suggestions. Comments from Jamie Shulmeister and two anonymous reviewers greatly improved this manuscript.

References

Alexander, D., T. Davies, and J. Shulmeister (2011), A steady-state mass-balance model for the Franz Josef Glacier, New Zealand: Testing and application, *Geogr. Ann., Ser. A*, *93*, 41–54, doi:10.1111/j.1468-0459.2011.00003.x.

Alloway, B., D. Lowe, D. Barrell, R. Newnham, P. Almond, P. Augustinus, N. Bertler, L. Carter, N. Litchfield, and M. McGlone (2007), Towards a climate event stratigraphy for New Zealand over the past 30,000 years (NZ-INTIMATE project), *J. Quat. Sci.*, *22*(1), 9–35, doi:10.1002/jqs.1079.

Anders, A., G. Roe, and B. Hallet (2006), Spatial patterns of precipitation and topography in the Himalaya, *Spec. Pap. Geol. Soc. Am.*, *398*, 39–53.

Anderson, B., and A. Mackintosh (2006), Temperature change is the major driver of late-glacial and Holocene glacier fluctuations in New Zealand, *Geology*, *34*(2), 121–124, doi:10.1130/G22151.1.

Anderson, B., and A. Mackintosh (2012), Controls on mass balance sensitivity of maritime glaciers in the Southern Alps, New Zealand: The role of debris cover, *J. Geophys. Res.*, *117*, F01003, doi:10.1029/2011JF002064.
Anderson, B., W. Lawson, and I. Owens (2008), Response of Franz Josef Glacier Ka Roimata o Hine Hukatere to climate change, *Global Planet. Change*, *63*, 23–30, doi:10.1016/j.gloplacha.2008.04.003.
Anderson, B., A. Mackintosh, D. Stumm, L. George, T. Kerr, A. Winter-Billington, and S. Fitzsimons (2010), Climate sensitivity of a high-precipitation glacier in New Zealand, *J. Glaciol.*, *56*(195), 114–128, doi:10.3189/002214310791190929.
Anderson, L. S., G. H. Roe, and R. S. Anderson (2014), The effects of interannual climate variability on the moraine record, *Geology*, *42*(1), 55–58, doi:10.1130/G34791.1.
Barrell, D., B. Andersen, and G. Denton (2011), *Glacial Geomorphology of the Central South Island, New Zealand*, *GNS Sci. Monogr.*, vol. 27, GNS Science, Lower Hutt, New Zealand.
Barrows, T., and S. Juggins (2005), Sea-surface temperatures around the Australian margin and Indian Ocean during the Last Glacial Maximum, *Quat. Sci. Rev.*, *24*, 1017–1047, doi:10.1016/j.quascirev.2004.07.020.
Barrows, T., S. Juggins, P. de Deckker, and E. Calvo (2007), Long-term sea surface temperature and climate change in the Australian–New Zealand region, *Paleoceanography*, *22*, PA2215, doi:10.1029/2006PA001328.
Bostock, H. C., et al. (2013), A review of the Australian–New Zealand sector of the Southern Ocean over the last 30 ka (Aus-INTIMATE project), *Quat. Sci. Rev.*, *74*, 35–57, doi:10.1016/j.quascirev.2012.07.018.
Braithwaite, R. J. (1995), Positive degree-day factors for ablation on the Greenland ice sheet studied by energy-balance modelling, *J. Glaciol.*, *41*(137), 153–160.
Burke, E. E., and G. H. Roe (2013), The absence of memory in the climatic forcing of glaciers, *Clim. Dyn.*, *42*, 1–12, doi:10.1007/s00382-013-1758-0.
Chinn, T. (1995), Glacier fluctuations in the Southern Alps of New Zealand determined from snowline elevations, *Arct. Alp. Res.*, *27*(2), 187–198.
Cox, S., and D. Barrell (2007), *Geology of the Aoraki Area 1:250,000, Geological Map 15*, GNS Science, Lower Hutt, New Zealand.
Cuffey, K., and W. Paterson (2010), *The Physics of Glaciers*, Butterworth Heinemann, Oxford.
Doughty, A. M., B. M. Anderson, A. N. Mackintosh, M. R. Kaplan, M. J. Vandergoes, D. J. A. Barrell, G. H. Denton, J. M. Schaefer, T. J. H. Chinn, and A. E. Putnam (2013), Evaluation of Late Glacial temperatures in the Southern Alps of New Zealand based on glacier modelling at Irishman Stream, Ben Ohau Range, *Quat. Sci. Rev.*, *74*, 160–169, doi:10.1016/j.quascirev.2012.09.013.
Drost, F., J. Renwick, B. Bhaskaran, H. Oliver, and J. McGregor (2007), A simulation of New Zealand's climate during the Last Glacial Maximum, *Quat. Sci. Rev.*, *26*(19–21), 2505–2525, doi:10.1016/j.quascirev.2007.06.005.
Glasser, N. F., K. Jansson, S. Harrison, and A. Rivera (2005), Geomorphological evidence for variations of the North Patagonian Icefield during the Holocene, *Geomorphology*, *71*(3–4), 263–277, doi:10.1016/j.geomorph.2005.02.003.
Golledge, N. R., and A. Hubbard (2009), Mass balance, flow and subglacial processes of a modelled Younger Dryas ice cap in Scotland, *J. Glaciol.*, *55*(189), 32–42, doi:10.3189/002214309788608967.
Golledge, N. R., A. Hubbard, and T. Bradwell (2010), Influence of seasonality on glacier mass balance, and implications for palaeoclimate reconstructions, *Clim. Dyn.*, *35*(5), 757–770, doi:10.1007/s00382-009-0616-6.
Golledge, N. R., A. N. Mackintosh, B. M. Anderson, K. M. Buckley, A. M. Doughty, D. J. A. Barrell, G. H. Denton, M. J. Vandergoes, B. G. Andersen, and J. M. Schaefer (2012), Last Glacial Maximum climate in New Zealand inferred from a modelled Southern Alps icefield, *Quat. Sci. Rev.*, *46*(C), 30–45, doi:10.1016/j.quascirev.2012.05.004.
Goodison, B. E. (1978), Accuracy of Canadian snow gauge measurements, *J. Appl. Meteorol.*, *17*(10), 1542–1548.
Griffiths, G., and M. McSaveney (1983), Distribution of mean annual precipitation across some steepland regions of New Zealand, *N. Z. J. Sci.*, *26*, 197–209.
Groisman, P. Y., and D. R. Legates (1994), The accuracy of United States precipitation data, *Bull. Am. Meteorol. Soc.*, *75*(2), 215–227.
Henderson, R., and S. Thompson (1999), Extreme rainfalls in the Southern Alps of New Zealand, *J. Hydrol.*, *38*(2), 309–330.
Herman, F., B. Anderson, and S. Leprince (2011), Mountain glacier velocity variation during a retreat/advance cycle quantified using sub-pixel analysis of ASTER images, *J. Glaciol.*, *57*(202), 197–207.
Hock, R. (2003), Temperature index melt modelling in mountain areas, *J. Hydrol.*, *282*(1–4), 104–115, doi:10.1016/S0022-1694(03)00257-9.
Hutter, K. (1983), *Theoretical Glaciology: Material Science of Ice and the Mechanics of Glaciers and Ice Sheets*, Reidel, Tokyo.
Ibbitt, R., R. Henderson, J. Copeland, and D. Wratt (2001), Simulating mountain runoff with mesoscale weather model rainfall estimates: A New Zealand experience, *J. Hydrol.*, *239*(1–4), 19–32.
Jarosch, A. H., C. G. Schoof, and F. S. Anslow (2013), Restoring mass conservation to shallow ice flow models over complex terrain, *Cryosphere*, *7*(1), 229–240, doi:10.5194/tc-7-229-2013.
Jóhannesson, T., C. Raymond, and E. Waddington (1989), Time-scale for the adjustment of glaciers to changes in mass balance, *J. Glaciol.*, *35*(121), 355–369.
Kaplan, M. R., P. I. Moreno, and M. Rojas (2008), Glacial dynamics in southernmost South America during Marine Isotope Stage 5e to the Younger Dryas chron: A brief review with a focus on cosmogenic nuclide measurements, *J. Quat. Sci.*, *23*(6–7), 649–658, doi:10.1002/jqs.1209.
Kaplan, M. R., J. M. Schaefer, G. H. Denton, D. J. A. Barrell, T. J. H. Chinn, A. E. Putnam, B. G. Andersen, R. C. Finkel, R. Schwartz, and A. M. Doughty (2010), Glacier retreat in New Zealand during the Younger Dryas stadial, *Nature*, *467*, 194–197, doi:10.1038/nature09313.
Kaplan, M. R., et al. (2013), The anatomy of long-term warming since 15 ka in New Zealand based on net glacier snowline rise, *Geology*, *41*(8), 887–890, doi:10.1130/G34288.1.
Kessler, M., and R. Anderson (2006), Modeling topographic and climatic control of east-west asymmetry in Sierra Nevada glacier length during the Last Glacial Maximum, *J. Geophys. Res.*, *111*, F02002, doi:10.1029/2005JF000365.
Laabs, B., M. Plummer, and D. Mickelson (2006), Climate during the last glacial maximum in the Wasatch and southern Uinta Mountains inferred from glacier modeling, *Geomorphology*, *75*(3–4), 300–317, doi:10.1016/j.geomorph.2005.07.026.
Le Meur, E., O. Gagliardini, T. Zwinger, and J. Ruokolainen (2004), Glacier flow modelling: A comparison of the Shallow Ice Approximation and the full-Stokes solution, *C. R. Phys.*, *5*(7), 709–722, doi:10.1016/j.crhy.2004.10.001.
MacGregor, K. R., R. S. Anderson, S. P. Anderson, and E. P. Waddington (2000), Numerical simulations of glacial-valley longitudinal profile evolution, *Geology*, *28*(11), 1031–1034.
McKinnon, K. A., A. N. Mackintosh, B. M. Anderson, and D. J. A. Barrell (2012), The influence of sub-glacial bed evolution on ice extent: A model-based evaluation of the Last Glacial Maximum Pukaki glacier, New Zealand, *Quat. Sci. Rev.*, *57*(C), 46–57, doi:10.1016/j.quascirev.2012.10.002.
Nelson, C., I. Hendy, H. Neil, and C. Hendy (2000), Last glacial jetting of cold waters through the Subtropical Convergence zone in the Southwest Pacific off eastern New Zealand, and some geological implications, *Palaeogeogr. Palaeoclimatol. Palaeoecol.*, *156*, 103–121.
Oerlemans, J. (1997), Climate sensitivity of Franz Josef Glacier, New Zealand, as revealed by numerical modeling, *Arct. Alp. Res.*, *29*(2), 233–239.
Oerlemans, J. (2001), *Glaciers and Climate Change*, 1st ed., A.A. Balkema, Lisse.

Oerlemans, J., B. Anderson, A. Hubbard, P. Huybrechts, T. Jóhannesson, W. Knap, M. Schmeits, A. Stroeven, R. van de Wal, and J. Wallinga (1998), Modelling the response of glaciers to climate warming, *Clim. Dyn.*, *14*(4), 267–274.

Plummer, M., and F. Phillips (2003), A 2-D numerical model of snow/ice energy balance and ice flow for paleoclimatic interpretation of glacial geomorphic features, *Quat. Sci. Rev.*, *22*(14), 1389–1406, doi:10.1016/S0277-3791(03)00081-7.

Porter, S. (1975), Equilibrium-line altitudes of late Quaternary glaciers in the Southern Alps, New Zealand, *Quat. Res.*, *5*(1), 27–47, doi:10.1016/0033-5894(75)90047-2.

Putnam, A. E., G. H. Denton, J. M. Schaefer, D. J. A. Barrell, B. G. Andersen, R. C. Finkel, R. Schwartz, A. M. Doughty, M. R. Kaplan, and C. Schlüchter (2010), Glacier advance in southern middle-latitudes during the Antarctic Cold Reversal, *Nat. Geosci.*, *3*(10), 700–704, doi:10.1038/ngeo962.

Putnam, A. E., J. M. Schaefer, G. H. Denton, D. J. A. Barrell, R. C. Finkel, B. G. Andersen, R. Schwartz, T. J. H. Chinn, and A. M. Doughty (2012), Regional climate control of glaciers in New Zealand and Europe during the pre-industrial Holocene, *Nat. Geosci.*, *5*(8), 1–4, doi:10.1038/ngeo1548.

Putnam, A. E., et al. (2013a), Warming and glacier recession in the Rakaia valley, Southern Alps of New Zealand, during Heinrich Stadial 1, *Earth Planet. Sci. Lett.*, *382*(C), 98–110, doi:10.1016/j.epsl.2013.09.005.

Putnam, A. E., J. M. Schaefer, G. H. Denton, D. J. A. Barrell, S. D. Birkel, B. G. Andersen, M. R. Kaplan, R. C. Finkel, R. Schwartz, and A. M. Doughty (2013b), The Last Glacial Maximum at 44°S documented by a ^{10}Be moraine chronology at Lake Ohau, Southern Alps of New Zealand, *Quat. Sci. Rev.*, *62*(C), 114–141, doi:10.1016/j.quascirev.2012.10.034.

Refsnider, K., B. Laabs, M. Plummer, D. Mickelson, B. Singer, and M. Caffee (2008), Last glacial maximum climate inferences from cosmogenic dating and glacier modeling of the western Uinta ice field, Uinta Mountains, Utah, *Quat. Res.*, *69*(1), 130–144, doi:10.1016/j.yqres.2007.10.014.

Reichert, B. K., L. Bengtsson, and J. Oerlemans (2002), Recent glacier retreat exceeds internal variability, *J. Clim.*, *15*, 3069–3081.

Roe, G. H. (2005), Orographic precipitation, *Annu. Rev. Earth Planet. Sci.*, *33*(1), 645–671, doi:10.1146/annurev.earth.33.092203.122541.

Roe, G. H. (2011), What do glaciers tell us about climate variability and climate change?, *J. Glaciol.*, *57*(203), 567–578, doi:10.3189/002214311796905640.

Roe, G. H., and M. A. O'Neal (2009), The response of glaciers to intrinsic climate variability: Observations and models of late-Holocene variations in the Pacific Northwest, *J. Glaciol.*, *55*(193), 839–854, doi:10.3189/002214309790152438.

Rother, H., and J. Shulmeister (2006), Synoptic climate change as a driver of late Quaternary glaciations in the mid-latitudes of the Southern Hemisphere, *Clim. Past*, *1*(3), 231–253, doi:10.5194/cp-2-11-2006.

Rowan, A. V., M. A. Plummer, S. H. Brocklehurst, M. A. Jones, and D. M. Schultz (2013), Drainage capture and discharge variations driven by glaciation in the Southern Alps, New Zealand, *Geology*, *41*(2), 199–202, doi:10.1130/G33829.1.

Schultz, D., et al. (2002), Understanding Utah winter storms: The Intermountain Precipitation Experiment, *Bull. Am. Meteorol. Soc.*, *83*(2), 189–210.

Shulmeister, J., T. R. Davies, D. J. A. Evans, O. M. Hyatt, and D. S. Tovar (2009), Catastrophic landslides, glacier behaviour and moraine formation—A view from an active plate margin, *Quat. Sci. Rev.*, *28*(11-12), 1085–1096, doi:10.1016/j.quascirev.2008.11.015.

Shulmeister, J., D. Fink, O. M. Hyatt, G. D. Thackray, and H. Rother (2010), Cosmogenic 10Be and 26Al exposure ages of moraines in the Rakaia Valley, New Zealand and the nature of the last termination in New Zealand glacial systems, *Earth Planet. Sci. Lett.*, *297*, 558–566.

Sinclair, M., D. Wratt, R. Henderson, and W. Gray (1997), Factors affecting the distribution and spillover of precipitation in the Southern Alps of New Zealand—A case study, *J. Appl. Meteorol.*, *36*(5), 428–442.

Steenburgh, W. (2003), One hundred inches in one hundred hours: Evolution of a Wasatch Mountain winter storm cycle, *Weather Forecast.*, *18*, 1018–1036.

Tait, A., R. Henderson, R. Turner, and X. Zheng (2006), Thin plate smoothing spline interpolation of daily rainfall for New Zealand using a climatological rainfall surface, *Int. J. Climatol.*, *26*(14), 2097–2115, doi:10.1002/joc.1350.

Tippett, J., and P. Kamp (1995), Geomorphic evolution of the Southern Alps, New Zealand, *Earth Surf. Processes Landforms*, *20*(2), 177–192.

Tovar, D., J. Shulmeister, and T. R. Davies (2008), Evidence for a landslide origin of New Zealand's Waiho Loop moraine, *Nat. Geosci.*, *1*(8), 524–526, doi:10.1038/ngeo249.

World Glacier Monitoring Service (WGMS) (2013), *Glacier Mass Balance Bulletin No. 12 (2010–2011)*, edited by M. Zemp et al., 106 pp., ICSU (WDS)/IUGG(IACS)/UNEP/UNESCO/WMO, World Glacier Monitoring Service, Zurich, Switzerland, doi:10.5904/wgms-fog-2013-11, publication based on database version.

Willett, S. (1999), Orogeny and orography: The effects of erosion on the structure of mountain belts, *J. Geophys. Res.*, *104*(B12), 28,957–28,981.

Woo, M., and B. Fitzharris (1992), Reconstruction of mass balance variations for Franz Josef Glacier, New Zealand, 1913 to 1989, *Arct. Alp. Res.*, *24*, 281–290.

Wratt, D., R. Ridley, M. Sinclair, H. Larsen, S. Thompson, R. Henderson, G. Austin, S. Bradley, A. Auer, and A. Sturman (1996), The New Zealand Southern Alps Experiment, *Bull. Am. Meteorol. Soc.*, *77*, 683–692.

Wratt, D., M. Revell, M. Sinclair, W. Gray, R. Henderson, and A. Chater (2000), Relationships between air mass properties and mesoscale rainfall in New Zealand's Southern Alps, *Atmos. Res.*, *52*(4), 261–282.

Yang, D., B. Goodison, S. Ishida, and C. Benson (1998), Adjustment of daily precipitation data at 10 climate stations in Alaska: Application of World Meteorological Organization intercomparison results, *Water Resour. Res.*, *34*(2), 241–256.

Zuo, Z., and J. Oerlemans (1997), Numerical modeling of the historic front variation and the future behavior of the Pasterze glacier, Austria, *Ann. Glaciol.*, *24*, 235–241.